FAST, ITERATIVE, FIELD-CORRECTED IMAGE RECONSTRUCTION FOR MRI

Bradley P. Sutton, Douglas C. Noll, Jeffrey A. Fessler

Dept. of Biomedical Engineering, University of Michigan

ABSTRACT

Magnetic field inhomogeneities cause distortions in the reconstructed images for non-cartesian k-space MRI (using spirals, for example). Several noniterative methods are currently used to compensate for the off-resonance during the reconstruction, but these methods rely on the assumption of a smoothly varying field map. Recently, iterative methods have been proposed that do not rely on this assumption and have the potential to estimate undistorted field maps, but suffer from prohibitively long computation times. In this abstract we present a min-max derived, time-segmented approximation to the signal equation for MRI that, when combined with the nonuniform fast fourier transform, provides a fast, accurate field-corrected image reconstruction.

1. INTRODUCTION

Differences in the magnetic susceptibility of adjacent regions within an object, which occur for example near air/tissue interfaces in the brain, lead to image distortions in non-cartesian k-space MRI (using spirals, etc.). Many methods have been proposed to correct for the field distortions during the reconstruction of the images [1, 2, 3, 4, 5]. Most of these methods rely on acquiring an accurate estimate of the field map, but the standard field map estimation technique is to use two images acquired at different echo times and assume that all of the off-resonance phase accrual occurs at the echo time [6]. Also, both images used to estimate the field map are distorted themselves. Once a field map is obtained, one method of correction, the conjugate phase method [1, 5], seeks to compensate for the phase accrual at each time point due to the off-resonance, relying on the assumption of a smooth field map. Time-segmented and frequency-segmented approximations exist for this to speed image reconstruction [1, 7]. For this method, since the field map exists in distorted image space, we cannot hope to recover a distortion-free image. Kadah, et al. [3] tried to overcome this problem with a noniterative scheme, SPHERE, by reconstructing distorted images and estimating distorted field maps and using those to synthesize cor-

rected k-space data. This method also relies on the assumption of a smoothly-varying field map.

Model-based iterative reconstruction methods have the potential to account for field maps that violate the smoothly varying assumption. The iterative reconstruction algorithm proposed in [8] not only shows improvements in corrections of the image over noniterative methods, but shows that such a method can be used to estimate more accurate field maps. Unlike standard reconstruction schemes which perform an operation to take k-space data and reconstruct an image (we will call this a back-projector), most iterative reconstruction methods require a forward-projector (given an estimate of the object and field map, form k-space data) and its transpose. The problem to date with iterative reconstruction methods is computation time, with reported values of computation time per iteration ranging into tens of minutes [8]. Recently, some work has been done to develop an accurate and fast Non-Uniform Fast Fourier Transform (NUFFT) [9, 10] and this method has been applied to MRI data with spiral k-space trajectories [11, 12]. However, this method by itself does not allow for the modeling of field inhomogeneity effects. In a manner similar to time-segmented conjugate-phase reconstructions [1], we propose a fast time-segmented forward projector, and its transpose, that takes into account field effects and uses the NUFFT. We examined interpolation coefficients for the time segmentation in a min-max framework to get a fast, accurate iterative reconstruction algorithm for field-corrected imaging.

2. THEORY

For simplicity we present a 1D derivation, but the concepts generalize easily to 2D and 3D. In MRI, the discretized signal equation is given by:

$$s(t) = \sum_{n=0}^{N-1} x_n e^{-i\omega_0(r_n)(t+T_E)} e^{-i2\pi(k(t)\cdot r_n)}, \qquad (1)$$

where $s(t)$ is the signal at time t during the readout, T_E is the echo time, x_n is a function of the object's magnetization at location r_n, $\omega_0(r_n)$ is the field inhomogeneity present at r_n, and $k_r(t)$ is the k-space trajectory. We measure noisy samples of this signal: $y_i = s(t_i) + \varepsilon_i$, or equivalently $y = Ax + \varepsilon$, where $a_{i,j} = e^{-i\omega_0(r_j)(t_j+T_E)} e^{-i2\pi k(t_i)r_j}$. Since MRI noise is Gaussian, we want to estimate the image x from the k-space data y by least squares, $\min_x \|y - $

$Ax\|$. We apply the iterative conjugate gradient algorithm for minimization, each iteration of which requires computing $A^*(y - Ax)$ where * denotes the complex conjugate transpose. Computing Ax is simply evaluating (1). We propose to combine the NUFFT approach and a version of time segmentation (with min-max temporal interpolation) to compute (1) rapidly and accurately.

For a time-segmented approximation of the signal equation, we break the acquisition window into $L - 1$ time segments of width τ and compute the signal equation, according to (1), at the L endpoints. We then interpolate over these endpoints to evaluate an approximation to the signal equation at intermediate time points,

$$
\hat{s}(t) = \sum_{l=0}^{L-1} a^*{}_l(t) \times
$$
$$
\sum_{n=0}^{N-1} \left[x_n e^{-i\omega_0(r_n)(\tau l + T_E)} \right] e^{-i2\pi(k(t) \cdot r_n)}, \quad (2)
$$

where $a_l(t)$ is the interpolation coefficient for the lth endpoint for time t. Notice in (2) that this is just sums of discrete fourier transforms (DFT) of the term in brackets weighted by the coefficients $a^*{}_l(t)$. The DFT can be performed quickly and accurately using an NUFFT [10]. Following a min-max derivation similar to [13, 10], one can show that the min-max interpolation coefficients $a_l(t)$ in (2) satisfy:

$$
a(t) = (G^*G)^{-1}G^*b(t), \quad (3)
$$

where

$$
[G^*G]_{l,l'} = \sum_{n=0}^{N-1} e^{-i\omega_0(r_n)\tau(l-l')},
$$
$$
[G^*b(t)]_l = \sum_{n=0}^{N-1} e^{i\omega_0(r_n)(t-\tau l)}, \quad (4)
$$

for $l, l' = 0, \ldots, L - 1$. Only $G^*b(t)$ depends on the specific time positions, so the $L \times L$ matrix $(G^*G)^{-1}$ needs only be computed once for a field map and L. Notice that spatial position is absent from this equation. This means that rather than the spatial distribution of the field inhomogeneity, the histogram of the field map determines (4). We approximated the computation of (4) by forming the histogram of the field map using N_B equal-sized bins along the range of the inhomogeneity. Let m_p be the number of pixels having an off-resonance frequency that falls into bin p with a center off-resonant frequency of ω_p, then we can rewrite (4) as

$$
[G^*G]_{l,l'} \approx \sum_{p=1}^{N_B} m_p e^{-i\omega_p \tau(l-l')},
$$

$$
[G^*b(t)]_l \approx \sum_{p=1}^{N_B} m_p e^{i\omega_p(t-\tau l)}. \quad (5)
$$

The equations in (5) can be efficiently computed via a Fourier transform of m_p. Besides using the histogram corresponding to the true field map in (5), a general histogram was used and the differences in interpolators and their errors were compared.

3. METHODS

A simulation study was performed to evaluate the maximum interpolation errorover a range of times, t. We compared a linear interpolator based on the two nearest endpoints to the time sample of interest, a Hanning window interpolator using only the two nearest endpoints (similar to that used in [1] for the back-projector problem), the min-max interpolator (3), an interpolator based on the min-max framework using the histogram of the field map calculated according to (5), and an interpolator using a flat histogram over the range [-100,100] Hz (Generic Histogram) also calculated using (5). Looking at the maximum error over number of time segments, a suitable L was chosen and the effect of iteration was examined by looking at the normalized root-mean-squared error (NRMSE) in the reconstructed image of the interpolated, time-segmented approach versus using the full signal equation (1). The time-segmented, NUFFT reconstruction scheme was then applied to a real data set collected on a 3.0T GE Signa Scanner in accordance with the Institutional Review Board of the University of Michigan. In the simulation and brain studies, a single-shot spiral k-space trajectory was used with a matrix size of 64, giving 4024 k-space points, and a T_E of 20 ms.

4. RESULTS

A simulation study was performed to examine the error of the five interpolators described in Section 3 over various numbers of time segments. The simulation object was derived from a reconstructed image and estimated field map from an actual brain scan and is shown in Figure 1. The maximum error over a range of time points is shown for 3 through 19 time segments ($L - 1$) in Figure 2. The min-max interpolators (ideal min-max, histogram min-max, and generic histogram min-max) have been plotted until the condition number of the (G^*G) matrix becomes too large for inversion. Notice that at $L = 9$ the max error for the min-max and histogram interpolator is nearly 4 orders of magnitude lower than that of the linear and Hanning. When a histogram of the field map is used that doesn't correspond to the actual field map (generic histogram), the max error shows this level of reduced error, but only when using a larger number of time segments.

The profiles of the interpolators are given in Figure 3 using $L = 6$ for the Hanning and min-max interpolators. The histogram interpolators looked very similar to the ideal min-max interpolator, even though the generic histogram

had a very different range of off-resonance and different histogram shape (flat). Even though it was not explicitly required, the min-max interpolators appear to sum to 1 at every time point.

Looking at the max error in Figure 2, we select $L = 9$ to give a low error for the min-max interpolator, and look at the error of time segmentation versus using the full signal equation (1) over iteration to see how the error propagates through the iterative process. As shown in Figure 4, the error is fairly stable over iteration for all of the interpolators.

For a comparison of computation time, Figure 5 shows the NRMSE vs computation time for $L = 4, \ldots, 10$. The time is given normalized to the time to evaluate the full signal equation. On a 700 MHz Pentium Workstation using Matlab (The Mathworks), the full signal equation took 15 sec. to evaluate. The min-max interpolation method, using various values of L, took around 10% of this time, with a normalized error on th order of 10^{-5}.

As a final comparison, we look at real data collected from a slice of the brain and reconstructed with both the proposed iterative method and a full conjugate phase method. Although the proposed iterative method can be used in an extended form to estimate an undistorted field map, in this case we were just comparing computation time, so both reconstructions used a field map obtained in the standard way. The iterative method used the generic histogram min-max interpolator since it does not depend on the field map and can be computed in advance for a given trajectory (depends only on number of time points and a chosen range of off-resonance frequencies). The NUFFT used an oversampling factor of 2 and a neighborhood size of 6 and the min-max interpolator used $L = 10$. The reconstruction time for the full conjugate phase was 6.96 s and the reconstruction time for five iterations of the proposed method was 5.45 s. The resulting reconstructions are shown in Figure 6. In practice, the iterative method can be used to simultaneously estimate an undistorted field map and provide a better field-corrected image, as evidenced in [8].

5. DISCUSSION

We have presented a method that allows fast, iterative reconstruction of field-corrected MRI images. By combining the NUFFT with time segmentation using a min-max temporal interpolator, a computation speed up of a factor of 10 is achievable with NRMSE on the order of 10^{-5} when compared to using the full signal equation. This method should easily be adaptable to other forms of iterative reconstruction in MRI, including multiple coil sensitivity encoding (SENSE).

6. REFERENCES

[1] D. C. Noll, C. H. Meyer, J. M. Pauly, D. G. Nishimura, and A. Macovski, ," *IEEE Trans. on Med. Im.*, vol. 10, no. 4, pp. 629–637, 1991.

[2] D. C. Noll, J. M. Pauly, C. H. Meyer, D. G. Nishimura, and A. Macovski, ," *Mag. Res. in Med.*, vol. 25, pp. 319–333, 1992.

[3] Y. M. Kadah and X. Hu, ," *Mag. Res. in Med.*, vol. 38, pp. 615–627, 1997.

[4] Y. M. Kadah and X. Hu, ," *IEEE Trans. on Med. Im.*, vol. 17, no. 3, pp. 362–370, 1998.

[5] H. Schomberg, ," *IEEE Trans. on Med. Im.*, vol. 18, no. 6, pp. 481–495, 1999.

[6] K. S. Nayak and D. G. Nishimura, ," *Mag. Res. in Med.*, vol. 43, pp. 151–154, 2000.

[7] L.-C. Man, J. M. Pauly, and A. Macovski, ," *Mag. Res. in Med.*, vol. 37, pp. 785–792, 1997.

[8] T. B. Harshbarger and D. B. Twieg, ," *IEEE Trans. on Med. Im.*, vol. 18, no. 3, pp. 196–205, 1999.

[9] A. Dutt and V. Rokhlin, ," *SIAM J. on Sci. Comp.*, vol. 14, no. 6, pp. 1368–1393, 1993.

[10] J. A. Fessler and B. P. Sutton, ," in *Proc. IEEE Intl. Conf. on Image Processing*, 2001, vol. 1, pp. 706–709.

[11] S. A. R. Kannengießer, J. M. Pauly, and R. K. Butts, ," in *ISMRM 9th Scientific Meeting*, 2001, p. 1800.

[12] B. Sutton, J. A. Fessler, and D. Noll, ," in *ISMRM 9th Scientific Meeting*, 2001, p. 763.

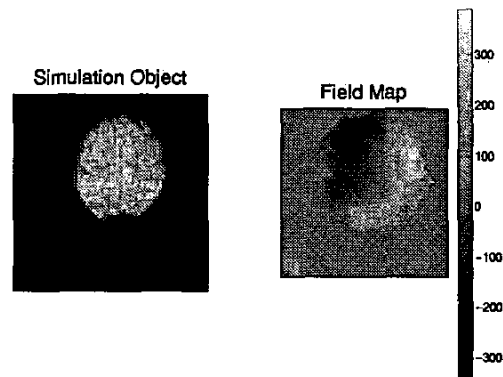[13] J. A. Fessler and B. P. Sutton, ," Submitted to IEEE Trans. Sig. Proc., Dec. 2001, 2001.

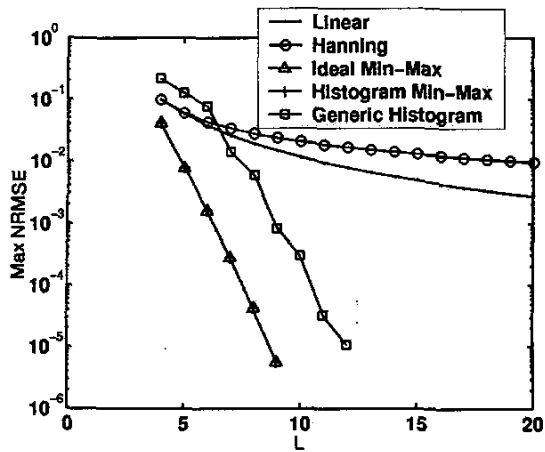**Fig. 1.** Simulation object (magnitude) and field map in rad/s.

Fig. 2. Maximum NRMSE over a range of time points for each interpolator for various numbers of time segments. Error is measured relative to full evaluation of the signal equation (1)
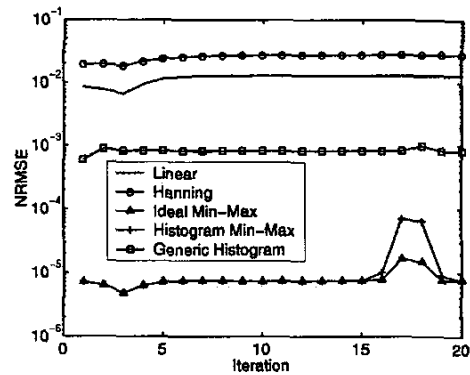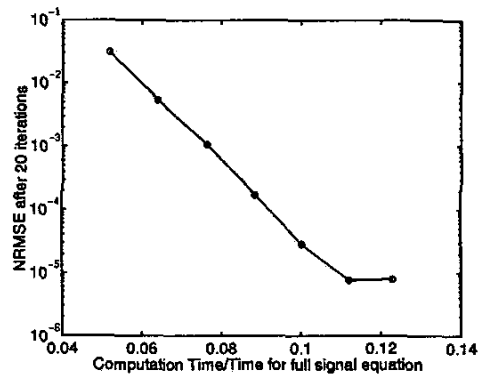

Fig. 4. NRMSE vs iteration for $L = 9$.

Fig. 5. NRMSE after 20 iterations vs. computation time for $L = 4, \ldots, 10$ for the ideal min-max interpolator. Time is given as a percentage of the computation time to evaluate the full signal equation (1).
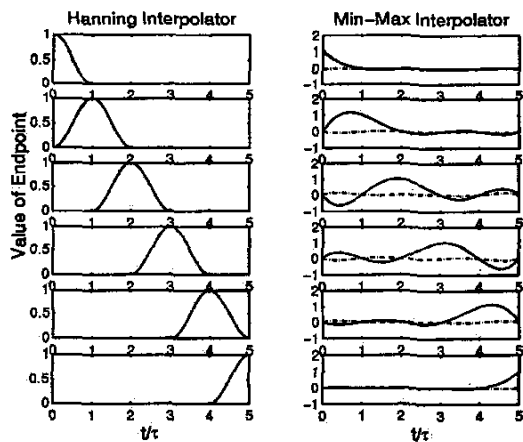

Fig. 3. Real (solid lines) and imaginary (dashed lines) parts of interpolators using $L = 6$ for the Hanning and min-max interpolators.
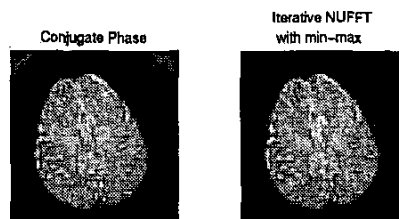

Fig. 6. Conjugate phase and iterative image reconstructions. The time for the full conjugate phase was 6.96 s and the time for five iterations of the iterative reconstruction was 5.45 s using $L = 10$.